Modeling the Fabrication Process of Micropatterned Macromolecular Scaffolds for Peripheral Nerve Regeneration

A. Sannino,[1] L. Silvestri,[2] M. Madaghiele,[1] B. Harley,[3,4] I. V. Yannas[3,4]

[1]*Department of Engineering for Innovation, University of Salento, Lecce 73100, Italy*
[2]*Department of Materials Science, University of Milano Bicocca, Via Cozzi 53, Milano I-20125, Italy*
[3]*Department of Mechanical Engineering, Massachusetts Institute of Technology, Cambridge, Massachusetts 02139*
[4]*Department of Biological Engineering, Massachusetts Institute of Technology, Cambridge, Massachusetts 02139*

Received 19 March 2009; accepted 1 November 2009
DOI 10.1002/app.31715
Published online 5 January 2010 in Wiley InterScience (www.interscience.wiley.com).

ABSTRACT: Tubular scaffolds demonstrated to be able to reconnect the proximal and distal stumps of transected peripheral nerves and induce regeneration of the lost nerve trunk. Recently, a spinning technique has been developed, able to produce tubular collagen-based scaffolds characterized by a radially patterned microporosity. The technique is based on the centrifugal sedimentation of collagen taking place when a cylinder, containing an aqueous collagen suspension, is rotated rapidly around its axis. In this work, the centrifugation process was modeled by means of the Lamm differential equation for collagen concentration, with the assumption that sedimentation and diffusion coefficients were dependent on the local concentration, according to appropriate scaling laws. With such assumptions, the model was able to predict the actual tube formation and its inner radius, in good agreement with the experimental results. The possibility to predict the final scaffold inner diameter as a function of the processing parameters has a fundamental importance for the set up of a precise fabrication method, which does not make use of any complex mold. This would significantly reduce the production complexity and the extent of scaffold manipulation during production, resulting in a cleaner production process and safety of the device. © 2010 Wiley Periodicals, Inc. J Appl Polym Sci 116: 1879–1888, 2010

Key words: biomaterials; centrifugation; modeling

INTRODUCTION

Regenerative medicine is a modern approach to treat severe injuries that spontaneously result in a repair healing mechanism characterized by wound closure via contraction and synthesis of scar tissue. Induced regeneration is a concept whereby a bioactive construct or scaffold is placed into the wound site, modifying the native healing mechanisms (repair) by inducing regeneration of physiological tissue.[1] There have been many studies of the regenerative capacity of the peripheral nervous system, following severe injuries.[1] In cases of complete transections of the nerve trunk, nerve autografts[1,2] represent the "old standard" reatment in neurosurgery, although autografts, even when available with appropriate length and thickness, induce a neurological deficit in the donor site without ensuring the full functional recovery of the injured nerve. The tissue engineering/regenerative medicine alternative to the use of autograft tissues is represented by the implantation of a tubular construct (termed conduit) between the proximal and distal stumps of the transected nerve, to bridge the nerve gap and provide directional guidance to the regrowing axons.[1] However, the extent and the quality of the resulting regeneration, in terms of bridgeable gap length and histological and conductive properties of the newly formed nerve trunk, compared to those of the native nerve, have been shown to be significantly affected by the microstructural, mechanical, compositional,and degradation features of the tubular construct itself, and of any material inserted within the tube lumen.[1,3–16]

Collagen has been identified as one of the most promising materials for the production of nerve guidance conduits, due to its biocompatibility and the observed enhanced cell attachment within collagen scaffolds.[8,12,13,17–20] The documented capability of collagen tubes to host myofibroblasts,[17] i.e., the cells responsible for the synthesis of scar tissue, might be one of the reasons for the high regenerative potential of these devices, if compared with analogue tubes based on synthetic polymers, notably polytetrafluoroethylene (PTFE),[21] poly(glycolic) acid (PGA),[1] lactic acid/ε-caprolactone based copolymer (LA/ε-CPL).[1,21]

Correspondence to: A. Sannino (alessandro.sannino@unisalento.it).

Porous polymeric tubes are usually produced by rolling and sealing the porous mesh of foam sheets, either by welding,[22] suturing,[23] gluing,[24] joining with solvent[25] or spraying over meshes.[26] Other techniques include various immersion precipitation methods[15] and, more recently, centrifugal casting.[27] In centrifugal casting, an impermeable cylindrical mold, containing a suspension of particles, is rapidly rotated around its longitudinal axis, so that centrifugal sedimentation of the particles toward the mold wall takes place. The size of the resulting tubular cast is function of the processing parameters, such as the spinning time and velocity. Moreover, when the contribution of diffusion to the flux of particles is not negligible compared to the centrifugal one, the cast wall shows a gradient of particle concentration, which results in a gradient of pore sizes in the final product. In case of multicomponent suspensions, different concentration profiles for the different particle types are obtained along the cast wall, leading to the formation of composites with given concentration gradients.

Although centrifugal casting is applied in many areas for the production of several devices, such as plastic pipes, ceramic supports[28] and functionally graded materials,[29,30] the use of such a technique for the production of nerve guidance conduits has not been largely explored.[27,31,32] However, centrifugal casting displays some peculiar advantages, if compared with other production processes, which make it attractive for the development of tissue engineering scaffolds. First of all, centrifuged tubes possess very smooth internal and external surfaces, which might provide better mechanical properties, a homogeneous cell attachment, and also make the handling and the suturing easier to the surgeon. Second, centrifuged tubes might show a radial gradient of pore sizes, which, if cell-permeable, might be exploited for a quantitative study of cell attachment and migration. Third, centrifugal casting can be exploited to produce tissue engineered tubular constructs, as cells can be homogeneously seeded into the scaffold while casting. For example, a similar process has been reported for the production of hydrogel-based, tissue engineered blood vessels.[33] Finally, several mathematical models of centrifugal casting can be developed, in order to predict the tube lumen formation, as well as the radial gradients in concentration (i.e., pore size)[30] and composition (i.e., in case of multicomponent casts[29]), as functions of the operating conditions.

A centrifugal casting technique for the production of collagen-based nerve guidance conduits has been recently reported[31] and patented.[34] Briefly, a collagen-chondroitin-6-sulfate suspension is injected into a plastic tube, which is then inserted into a cylindrical copper mold. The mold is spun with a given velocity around its axis for a certain time, and then immersed in liquid nitrogen, while spinning, for a rapid freezing of the spun suspension. The plastic tube containing the frozen suspension is then rapidly placed into a freeze dryer, to obtain the dry collagen tubular scaffolds. As expected, the conduits formed at high rotational velocities display a gradient in porosity and pore size along the tube radius, with a cell-permeable inner wall and a cell-impermeable outer wall, and a radially oriented pore pattern, due to the combined effect of centrifugal sedimentation and radial heat transfer during the freezing. Several collagen tubular scaffolds could be produced by varying the rotational velocity and the spinning time.[31]

The need to define the processing parameters meeting a specific lumen size and tube microstructure, in order to design and set-up a proper standardized production process, prompted this study to produce a mathematical model able to describe the sedimentation of the collagen phase during the spinning process. Centrifugal casting processes similar to that concerned in this work have been reported and modeled by Biesheuvel et al.,[28] although referring to ceramic suspensions. By calculating the settling velocity of ceramic particles during centrifugation, taking into account some correction factors for the dependence of the sedimentation coefficient on the concentration, those models were able to predict the cast thickness, its formation time and its concentration. It is worth noting that, as the diffusional contribution to mass transport could be neglected, due to the strong interactions among particles in the ceramic cast, no concentration gradient could be observed along the cast thickness.

The model proposed in this work for the centrifugal casting of collagen is based on the Lamm differential equation[35] for collagen concentration, which takes into account both the centrifugal and the diffusional contributions to the mass transport. In particular, the experiments showed that collagen tubes with a significant gradient of collagen concentration along the tube wall could be produced when adopting high rotational velocities. Making the basic assumption that sedimentation and diffusion coefficients are dependent on the local concentration, according to appropriate scaling laws, we were able to explain the observed tube formation after a given spinning time and predict the actual tube lumen diameters resulting from different processing parameters (i.e., spinning times and velocities). Results showed a good agreement between the model predictions and the experimental findings.

THEORETICAL BACKGROUND AND MATHEMATICAL MODELING

The fabrication technique used here to induce the collagen tube formation can be described by the

same approach commonly adopted in sedimentation analysis. The general features of our experimental method can be understood in that framework. During the spinning of the collagen suspension at a given rotor speed ω, three forces act on the solid phase (i.e., collagen and chondroitin-6-sulfate molecules) due to the fast rotation (Fig. 1), respectively a centrifugal force f_c, a frictional force f_f, and an Archimedeal or buoyant force f_a. The effect of gravity is negligible compared to that of centrifugation (being $\omega^2 r/g \gg 1$), so that solid particles move only in the radial direction. At low rotor speeds, our procedure resembles an equilibrium centrifugation experiment, in which a balance between sedimentation and diffusion is reached, producing a stationary concentration profile inside the rotor. At higher rotor speeds and/or spinning times, sedimentation dominates and we observe the formation of a sharp boundary between the nearly pure liquid and the solid phase; we will indicate this regime as ultra centrifugation. In this case, the solid phase is completely removed from the central part of the cylindrical mold, leading to the formation of a tubular collagen structure after the freeze drying process.

If we consider collagen-chondroitin-6-sulfate copolymer as a single species, then our system can be completely described by the concentration $c(r,t)$ of such a polymer at every time as a function of the radial distance from the cylinder axis. The basic differential equation governing sedimentation behavior has been derived by Lamm[35]:

$$\frac{\partial c}{\partial t} = -\frac{1}{r}\frac{\partial}{\partial r}[rJ(r,t)] = \frac{1}{r}\frac{\partial}{\partial r}\left[rD\frac{\partial c}{\partial r} - s\omega^2 r^2 c\right] \quad (1)$$

where s and D are the solute sedimentation and cooperative diffusion coefficients respectively, and $J(r,t)$ is the solute transport flux. If the initial concentration profile is uniform along the cylinder radius, then the initial condition accompanying eq. (1) will be:

$$c(r,0) = c_0 = \text{const} \quad (2)$$

In our case, c_0 corresponds to the initial concentration of the collagen-based slurry. The appropriate boundary conditions are given by the vanishing of the flux at both the cylinder boundary and axis, i.e., $J(R,t) = J(0,t) = 0$:

$$J(R,t) = \left[rD\frac{\partial c}{\partial r} - s\omega^2 r^2 c\right]_{r=R} = 0 \quad (3)$$

$$J(0,t) = \lim_{r\to 0}\left[rD\frac{\partial c}{\partial r} - s\omega^2 r^2 c\right] = 0 \quad (4)$$

with R being the radius of the cylindrical mold containing the collagen suspension.

The Lamm equation can be solved only through numerical methods.[36,37] In this work, solutions to the Lamm equation were computed with the free software SEDFIT, which implements the moving grid method.[36] In numerical calculations, we have replaced the condition $J(0,t) = 0$ with $J(r_f,t) = 0$, where r_f is a constant value, comparable with the size of the collagen microfibrils. This approximation is useful for the calculations and it also makes physical sense since we know that solvent is always present between microfibrils.

Analytical solutions to the Lamm equation can be obtained in some special cases of practical importance. When the sedimentation process reaches the steady state (i.e., $\frac{\partial c}{\partial t} = 0$), the stationary concentration profile can be obtained by equating the flux to 0 everywhere and it is given by,

$$c(r,\infty) = c_0 \frac{R^2/2\beta^2}{\exp\left(R^2/2\beta^2\right) - 1}\exp\left(r^2/2\beta^2\right) \quad (5)$$

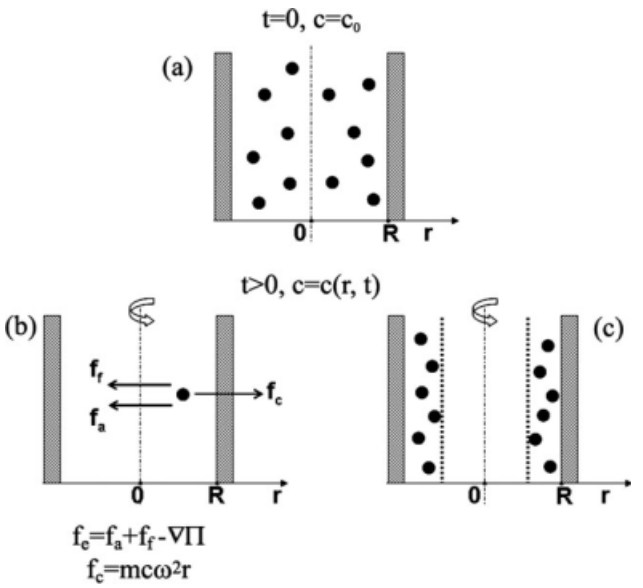

Figure 1 (a) Collagen-based suspension injected into the cylindrical mold: the initial concentration is uniform, with $c = c_0$. As the cylindrical mold is rotated along its longitudinal axis (b and c), a concentration profile $c(r,t)$ is obtained. (b) Three forces act on the single solid particle of the collagen-based suspension during rotation: f_c is the centrifugal force per unit volume, with m the mass of a collagen particle, and c the collagen concentration, expressed in particles per unit volume; f_e is the elastic force opposing f_c and tending to restore the uniform concentration, which results from the contributions of the frictional force f_f, the buoyant force f_a, and the osmotic pressure gradient $\nabla\Pi$. (c) Effect of the extreme sedimentation acting on the collagen molecules: an inner lumen devoid of solid particles is formed.

with

$$\beta = \sqrt{\frac{D}{s\omega^2}} \tag{6}$$

and c_0 the initial uniform concentration [see appendix for derivation of eq. (5)].

In equilibrium regime $\beta \approx R$, so that the concentration profile provided by eq. (5) is nearly uniform, while in the ultra centrifugation regime $\beta \ll R$ and we observe sedimentation of most of the collagen phase at the boundary.

However, the derivation of eq. (5) is based on the wrong assumption that s and D are constant. In fact, de Gennes[38] has shown that, for long flexible molecules in the semi-dilute and concentrated solutions, the following relations for s and D are valid:

$$s \propto c^{-\frac{1}{2}} \tag{7}$$

$$D \propto \xi^{-1} \tag{8}$$

where ξ is a correlation length that can be interpreted as the mesh size of the temporary network formed by the overlapping molecules, or, in our case, as the pore size. It can also be proved that $\xi \propto c^{-3/4}$ for semi-dilute solutions and $\xi \propto c^{-1/2}$ in concentrated ones. A straightforward generalization of our model, which is also easy to treat analytically, is obtained assuming:

$$s = s' c^{\sigma} \tag{9}$$

$$D = D' c^{\delta} \tag{10}$$

In this case, the shape of the stationary solutions of the corresponding Lamm equation will depend only on the exponent $\varepsilon = \delta - \sigma$ and will have the form:

$$c(r, \infty) = \left[\varepsilon\left(\frac{r^2}{2\beta'^2} + k\right)\right]^{1/\varepsilon} \tag{11}$$

where β' is given by:

$$\beta' = \sqrt{\frac{D'}{s'\omega^2}} \tag{12}$$

and k is a normalization constant. It can be shown that a proper normalization for the above stationary functions can be found only when the solute concentration is 0 up to a critical radial distance r_0 from the cylinder axis:

$$r_0 = R\sqrt{1 - \left(\frac{2\beta'^2}{R^2}\right)^{\frac{1}{\varepsilon+1}} \frac{(1+\varepsilon)^{\frac{\varepsilon}{\varepsilon+1}}}{\varepsilon}} \tag{13}$$

The value of r_0 can therefore be interpreted as the minimum radius of the lumen formed at equilibrium [see appendix for derivation of eqs. (10) and (12)]. The tube with the smallest lumen is finally described by:

$$c(r, \infty) = \begin{cases} 0 & \text{for } r \le r_0 \\ \left[\varepsilon\left(\frac{r^2 - r_0^2}{2\beta'^2}\right)\right]^{1/\varepsilon} & \text{for } r > r_0 \end{cases} \tag{14}$$

EXPERIMENTAL PROCEDURES

The collagen scaffolds were prepared using a three-step process which included: (1) preparation of a collagen-based slurry; (2) spinning of the slurry in a proper apparatus and rapid freezing of the sedimented suspension; (3) freeze drying of the solidified suspension to obtain the final scaffold. A complete and detailed description of this process has been reported in recent literature.[31] In the following, we report the fundamental information required for the mathematical modeling.

Preparation of collagen-based slurry

Type I microfibrillar collagen from bovine tendon was obtained from an industrial source (Integra LifeSciences Corporation, Plainsboro, NJ). A collagen dispersion (0.5 wt %) was prepared by mixing collagen granules and chondroitin-6-sulfate (0.05 wt %) isolated from shark cartilage (Sigma-Aldrich Chemical Co., St. Louis, MO) in 0.05*M* acetic acid (pH 3.2) using a rotor mixer or a plasticating extruder.

Spinning procedure and freeze drying

The collagen suspension was injected into a PVC tube (OD: 7.94 mm, ID: 4.76 mm, VWR Scientific Inc., West Chester, PA) that was inserted into a copper mold.[31] The copper mold was spun using a rotary tool (Dremel) for a specified length of time (T_s) at specified rpm setting (ω). The spinning mold was immersed (maintaining spinning velocity) into a liquid nitrogen bath. The collagen dispersion was frozen while spinning for the specified freezing time (T_f). The mold was then removed from liquid nitrogen and the spinning was stopped. The PVC tube containing the frozen dispersion was removed quickly from the copper mold and placed into the freeze-dryer (Genesis, VirTis, Inc., Gardiner, NY), which had been pre-set to −40°C. The frozen collagen suspension was then sublimated at a temperature of 0°C for 17 h at a pressure of 200 mTorr. The collagen scaffold was then removed from the PVC tube, placed into an aluminum foil packet and stored in a desiccator for further analysis. Two

TABLE I
Fabrication Conditions and Tube Lumen Diameter of Four Different Scaffolds Fabricated Using the Spinning Technique (T_s = Spinning Time in air; T_f = Spinning Time in the Liquid Nitrogen Bath; ω = Rotation Velocity)

ω (rpm)	T_s (min)	T_f (min)	Tube I.D. ± SD (mm)
5000	0	1	0
5000	3	1	0
5000	5	1	2.36 ± 0.01
30,000	15	2	3.14 ± 0.06

spinning velocities and three spinning times were employed during the tests (Table I), to analyze the effect of those parameters on the centrifugal casting of collagen. Experiments were performed in triplicate.

Morphological analysis

The pore structure and the lumen of the collagen tubes were assessed by means of scanning electron microscopy (SEM). Two cross-sections from distinct regions of each device were visualized using a VP438 Scanning Electron Microscope (Leo, Inc., UK).

RESULTS AND DISCUSSION

Four distinct scaffold structures were analyzed, as reported in Table I, and good experimental reproducibility was observed. When placing the mold containing the collagen suspension directly in liquid nitrogen [Fig. 2(a), $T_s = 0$ min], a cylindrical (filled) scaffold devoid of any specific pore orientation and with no evidence of sedimentation was produced. When spinning the mold in air at ω = 5000 rpm for $T_s = 3$ min [Fig. 2(b)], a cylindrical (filled) scaffold structure was still obtained. However, a radially aligned pore structure could be appreciated, showing also a lower concentration of the solid phase in the center of the scaffold (i.e., lower relative density represented by darker regions under SEM backscatter detectors). Both the radial pore alignment and the lower collagen concentration in the center of the scaffold can be explained considering the increased sedimentation effect due to centrifugation. If further increasing the spinning time to $T_s = 5$ min, while keeping ω constant [Fig. 2(c)], a tubular scaffold with a well-defined lumen (with a measured radius of about 1.2 mm) was obtained, due to a significant sedimentation, which totally removed the solid phase from the center of the cylindrical mold. Radial pore orientation, due to the combined effect of sedimentation and heat transfer gradient along the mold radius during the freezing, was observed for this class of tubular devices. However, no significant gradient of collagen concentration could be detected along the tube wall thickness. Further increasing the spinning time and velocity (ω = 30,000 rpm, $T_s = 15$ min) led to the formation of a collagen tube with a greater lumen [Fig. 3(a)], due to an extreme sedimentation effect. This type of device showed a peculiar microporous structure. Indeed, a radially aligned porosity pattern, with a pore size of ~ 20 μm [Fig. 3(b)], could be appreciated along the entire tube

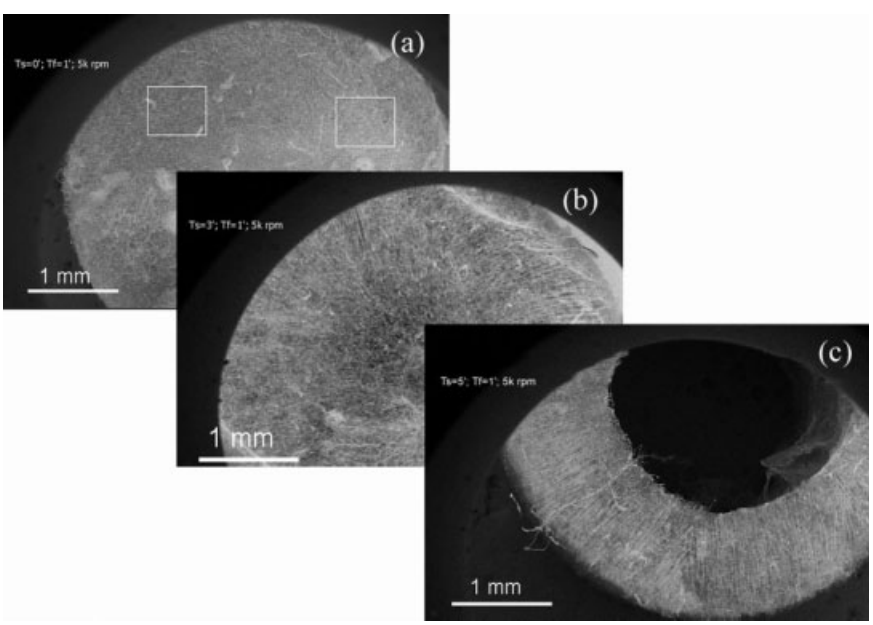

Figure 2 Cross-sectional SEM images of distinct classes of tubular scaffolds (filled or hollow) fabricated using distinct spinning protocols: (a) $T_f = 1$ min, $T_s = 0$ min, ω = 5000 rpm; (b) $T_f = 1$min, $T_s = 3$ min, ω = 5000 rpm; (c) $T_f = 1$min, $T_s = 5$ min, ω = 5000 rpm.

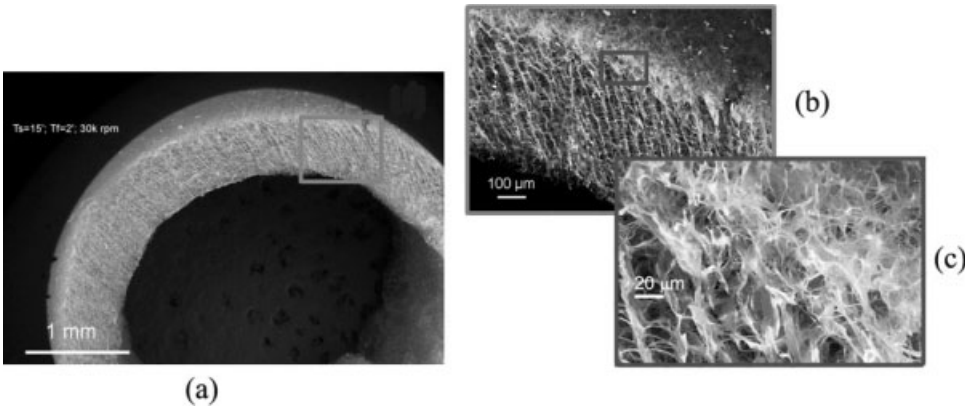

Figure 3 Cross-sectional SEM image (a) of the entire tube wall of a single scaffold fabricated using $T_f = 2$ min, $T_s = 15$ min, $\omega = 30{,}000$ rpm; (b) the radially aligned porosity pattern can be appreciated; (c) the outermost regions of the tube wall show a compacting effect of the solid phase on the tube wall, due to high sedimentation effect.

wall, with the exception of a small region near the outer edge of the tube, where the pores were not oriented and significantly smaller (<5 μm) [Fig. 3(c)]. Such small pores are likely ascribed to the compacting of collagen on the wall of the cylindrical mold, taking place during the extreme sedimentation process, and make the device cell-impermeable from the outside, while cells can still migrate into it from the interior tube lumen. These specific porous structures might be useful in studying the migration patterns of myofibroblasts during peripheral nerve regeneration.

To set up a fabrication method for the production of nerve guidance conduits, matching the requirements of different animal models as well as different "target" nerves, the aim of this work was to develop a mathematical model for the centrifugal casting of collagen, so that the lumen of the tubular devices can be predicted as a function of the operating conditions (i.e., spinning time and velocity). For the validation of the centrifugation model proposed earlier, which is based on the Lamm equation commonly adopted in sedimentation analysis, we need to estimate the ratio s/D. From our experiments, we could find that, for $T_s = 5$ min, a filled cylinder was obtained by spinning at $\omega = 2500$ rpm, while at $\omega = 5000$ rpm a hollow tube was formed. We can therefore estimate the order of magnitude of the ratio s/D by imposing that $R^2/2\beta^2 = 1$ at the critical speed $\omega_c = 2500$ rpm; recalling that the radius of the cylindrical mold is $R = 2.38$ mm, we finally obtain,

$$\frac{s}{D} = \frac{2}{R^2\omega_c{}^2} = 5.2 \times 10^{-4}\mathrm{s}^2\mathrm{cm}^{-2} \qquad (15)$$

Using the aforementioned relation, the stationary concentration profiles provided by eq. (5) were evaluated for different rotor speeds (Fig. 4). It is evident that the profile obtained at 2500 rpm describes a filled cylinder, whereas at 30,000 rpm we predict the formation of tube with a very large lumen. The intermediate case at 5000 rpm (solid line) is more difficult to handle. It is useful to define a critical concentration c^*, below which the solution is so dilute, that the freeze-drying procedure removes all the solid phase. Assuming $c^* = 0.25c_0$ for instance, we would predict the formation of a tube with an inner radius of about 1.3 mm. In the same spirit, we can find the explicit values of s and D from the experimental observation that, at 5000 rpm, the hollow region appears after 5 min. Assuming $s = 10^5$ S and $D = 192\times10^{-7}$ cm^2 s^{-1}, we can numerically solve the Lamm equation to obtain the time dependent concentration profiles displayed in Figure 5, where it is shown that, at 5000 rpm, the concentration drops below $0.25c_0$ after 5 min. This simplified model is

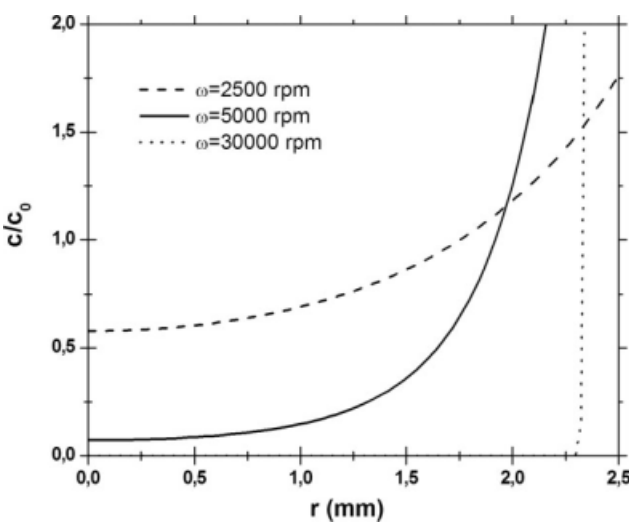

Figure 4 Equilibrium concentration profiles computed for $s/D = 5.2 \times 10^{-4}$ cm^{-2} s^2 and $\omega = 2500$ (dashed line), $\omega = 5000$ (solid line) and $\omega = 30{,}000$ (dotted line) rpm.

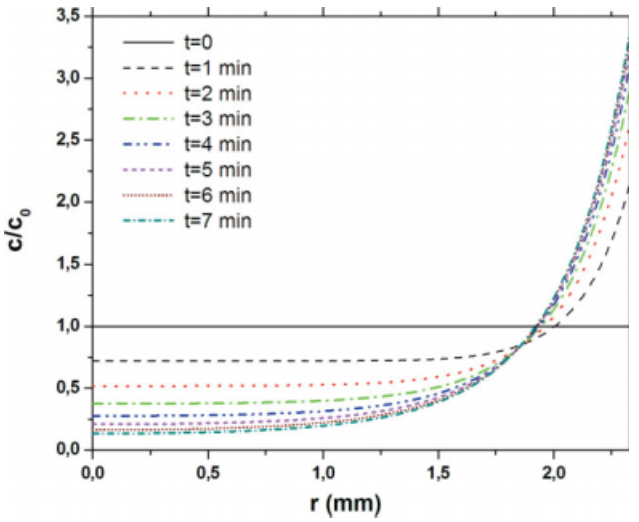

Figure 5 Time dependent concentration profile for $s = 10^{-8}$ s, $D = 192 \times 10^{-7}$ cm^2 s^{-1} and $\omega = 5000$ rpm. [Color figure can be viewed in the online issue, which is available at www.interscience.wiley.com.]

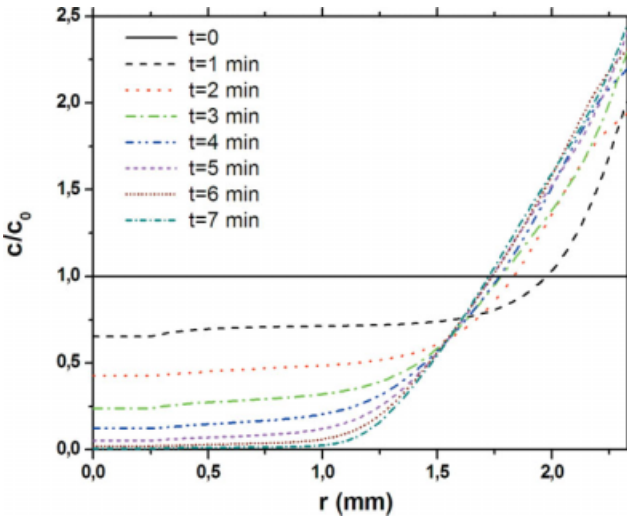

Figure 7 Time-dependent concentration profile for $s(c) = 10^{-9}$ $(0.1 + c/c_0)^{-17/2}$ s, $D(c) = 192 \times 10^{-4}$ $(0.1 + c/c_0)^{3/4}$ cm^2 s^{-1} and $\omega = 5000$ rpm. [Color figure can be viewed in the online issue, which is available at www.interscience.wiley.com.]

able to explain the general behavior of our system. It allows to predict the sedimentation behavior of collagen at low rotor speeds ($\omega \leq 5000$ rpm) and low spinning times ($T_s < 5$ min), which yield cylindrical or filled collagen scaffolds with a radial concentration gradient and radial pore patterns [Fig. 2(b)]. The model also provides an approximate estimation of the tube lumen formed at low rotor speeds [Fig. 2(c) and Table I vs. Fig. 4]. However, it is evident that the model fails at high rotor speeds (e.g., $\omega =$ 30,000 rpm), as it predicts an excessive accumulation of material at the boundary and does not estimate the actual tube lumen size [Fig. 3(a) and Table I vs. Fig. 4].

A more accurate model of the collagen centrifugation process is obtained by considering that s and D are functions of the local concentration, according to eqs. (9) and (10), respectively. The equilibrium concentration profiles provided by eq. (14) were evaluated for both $\omega = 5000$ rpm and $\omega = 30{,}000$ rpm, using the de Gennes values of the exponent, i.e., $\varepsilon =$

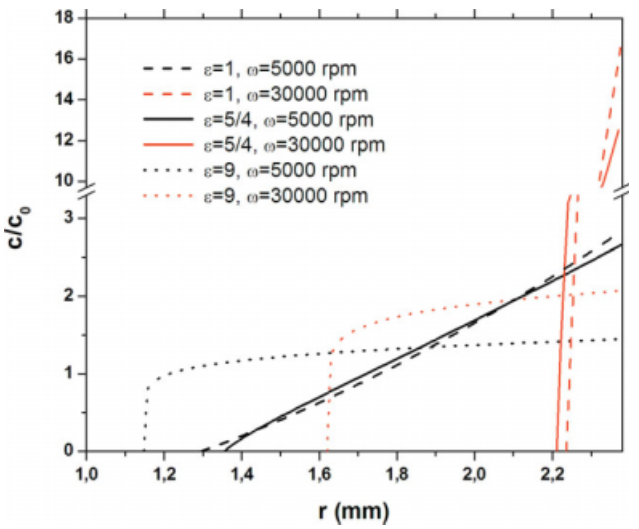

Figure 6 Equilibrium concentration profiles computed for $s(c)/D(c) = 5.2 \times 10^{-4} c^{\varepsilon}$ cm^{-2} s^2 and $\varepsilon = 1$ (dashed lines), $\varepsilon = 5/4$ (solid lines), and $\varepsilon = 9$ (dotted lines). For each value of the exponent, we report the equilibrium concentrations at $\omega = 5000$ (black lines) and $\omega = 30{,}000$ rpm (red lines). [Color figure can be viewed in the online issue, which is available at www.interscience.wiley.com.]

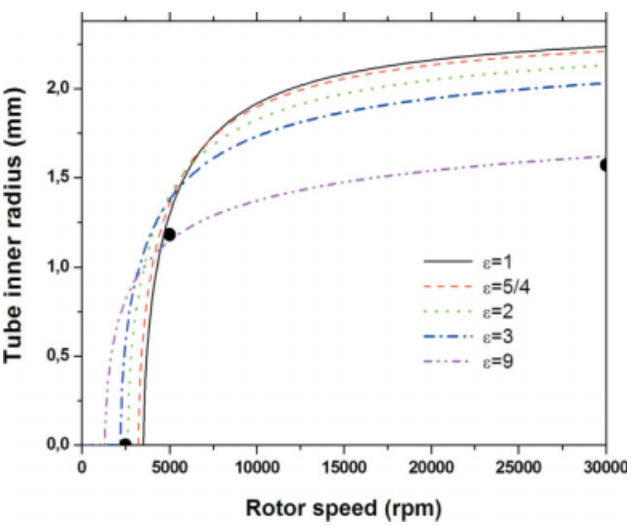

Figure 8 Predicted lumen radius at equilibrium for $s(c)/D(c) = 5.2 \times 10^{-4} c^{\varepsilon}$ cm^{-2} s^2 and different values of the exponent ε. Experimental data are reported as filled circles. [Color figure can be viewed in the online issue, which is available at www.interscience.wiley.com.]

5/4 and $\varepsilon = 1$ for semi-dilute and concentrated solutions respectively, as well as $\varepsilon = 9$ for the sake of comparison (Fig. 6). The full solution of the time dependent Lamm equation at $\omega = 5000$ rpm and $\varepsilon = 5/4$ was computed, for $s(c) = 10^{-9}\ (0.1+c/c_0)^{-1/2}$ s and $D(c) = 192 \times 10^{-4}\ (0.1+c/c_0)^{3/4}$ cm^2 s^{-1}, where the constant 0.1 inside round brackets was introduced to obtain a finite value at zero concentration (Fig. 7). The results of the calculations were found to agree very well with the experimental findings. The formation of a collagen cylindrical matrix was predicted for $T_s \leq 3$ min [Fig. 2(b)], whereas a collagen tube with a lumen radius of about 1.3 mm was predicted for $T_s = 5$ min [Fig. 2(c)]. In order to estimate the lumen size as a function of the rotor speed during the spinning, we also computed the dependence of r_0 from ω for different values of the exponent ε (Fig. 8), according to eq. (13). We found that, at low rotor speeds, the mathematical model of collagen sedimentation provided by eqs. (13) and (14) works well with values of ε between 0 and 2, in agreement with the de Gennes scaling laws (Figs. 6 and 8). Using those values of ε, the model predicts the actual size of the lumen formed at low rotor speeds, and also provides a better estimation of the concentration profile established along the collagen tube wall, if compared to the simplified model described by eq. (5) (Figs. 4 and 6). Conversely, at high rotor speeds, the correct ε to be used in the model seems to be about 9 (Fig. 8). With such a value of ε, the model is able to estimate the actual tube lumen formed at high rotational velocities, although the computed collagen concentration profile along the tube wall thickness (dotted lines, Fig. 6) does not explain the peculiar pore size gradient found experimentally, with cell-permeable pores on the inner regions vs. cell-impermeable pores on the outer edge of the collagen tube [Fig. 3(b,c)]. As explained earlier, the small pore size at the outer edge of the tube is due to the high concentration of collagen in this region, as a consequence of the extreme sedimentation protocol and the compacting of collagen on the wall of the cylindrical mold. A possible explanation for the unexpected value of ε is that, at high rotational speeds, the concentration at the cylinder boundary becomes so large that the same scaling laws derived for solutions do not describe collagen properties anymore. At the same time, the extremely high values of collagen concentration found only in the proximity of the cylinder boundary suggest that the use of a single ε value might be a source of error in the prediction of the actual concentration profile. More experimental data would be necessary to test such hypotheses and to refine the model.

On the overall, the results of this study showed that the Lamm equation for collagen concentration allows a good modeling of the centrifugal casting of collagen, as the computed predictions are consistent with the experimental findings. Although more accurate models should be developed for a deeper understanding of the sedimentation mechanisms of collagen molecules, especially at the boundary of the mold, the proposed model suffices to describe the formation of collagen tubes by centrifugal casting, thus providing the scientific basis for the design of centrifugal processes for the production of collagen-based nerve guidance conduits of desired size.

CONCLUSIONS

A mathematical model for the centrifugal casting of collagen suspensions was investigated. Centrifugal casting has been recently described as a technique able to produce collagen-based tubular devices characterized by a radially patterned microporosity, a cell-permeable inner wall, and a cell-impermeable outer wall. Such devices thus show potential as nerve guidance conduits in studies evaluating the migration patterns of myofibroblasts during the regeneration of peripheral nerves. The proposed model for centrifugal casting is based on the Lamm differential equation for collagen concentration, with the assumption that sedimentation and diffusion coefficients are dependent on the local concentration, according to appropriate scaling laws. With such assumption, the model was able to predict the actual collagen tube formation and its inner radius, and good agreement was obtained comparing the model data with the experimental results. This is of interest for the understanding of the phenomena related to the scaffold design under the selected experimental conditions as well as for the appropriate scale up of a precise fabrication procedure, avoiding the use of any complex mold.

APPENDIX: DERIVATION OF STATIONARY CONCENTRATION PROFILES FOR EITHER CONSTANT OR CONCENTRATION-DEPENDENT *S* AND *D*

In case of steady-state sedimentation, the Lamm equation [eq. (1)] results in the following:

$$rD\frac{\partial c}{\partial r} - s\omega^2 r^2 c = 0 \tag{A1}$$

Assuming that s and D are constant and recalling eq. (6) for the expression of β, the solution to the above differential equation is in the form:

$$c(r,\infty) = \exp\left(\frac{r^2}{2\beta^2}\right) \times K \tag{A2}$$

where K is a constant. The value of K can be calculated by considering the mass conservation rule in the cylindrical coordinate system, written as follows:

$$\int_0^R c(r) r dr = \text{const at any time t} \tag{A3}$$

and by assuming that the initial concentration profile is uniform along the cylinder radius (i.e., $c(r,0) = c_0$):

$$\int_0^R c(r) r dr = K \int_0^R \exp\left(\frac{r^2}{2\beta^2}\right) r dr = c_0 \frac{R^2}{2} \tag{A4}$$

By solving eq. (A4) for K and substituting the calculated value of K in eq. (A2), the concentration profile provided by eq. (5) is obtained:

$$c(r,\infty) = c_0 \frac{R^2/2\beta^2}{\exp\left(R^2/2\beta^2\right) - 1} \exp\left(r^2/2\beta^2\right)$$

The aforementioned model works well for low rotational velocities, i.e., in cases where β is comparable to R, so that the concentration profile is almost uniform along the cylinder radius. When $\beta \ll R$, as in the ultra centrifugation regime, the concentration gradient along the radius becomes significant. Considering that s and D are concentration-dependent, according to eqs. (9) and (10) respectively, eq. (A1) can be rewritten as:

$$r \frac{\partial c}{\partial r} - \frac{s'}{D'} \omega^2 r^2 c^{1-\varepsilon} = 0 \tag{A5}$$

The analytical solution of eq. (A5) is provided by eq. (11), which is rewritten in the following for the reader's convenience:

$$c(r,\infty) = \left[\varepsilon\left(\frac{r^2}{2\beta'^2} + k\right)\right]^{1/\varepsilon}$$

Here β' is defined by eq. (12), whereas k is a constant to be determined by considering the mass conservation expressed by eq. (A3).

As the ultra centrifugation results in the formation of hollow tubes, the value of the constant k can be expressed as in the following, by considering that the concentration is equal to 0 up to a certain radius r_0, whereas for $r_0 \le r \le R$ eq. (11) is valid:

$$k = -\frac{r_0^2}{2\beta'^2} \tag{A6}$$

In case of an initial uniform concentration profile equal to unity, k is a normalization constant and the mass conservation rule leads to:

$$\varepsilon^{1/\varepsilon} \int_{r_0}^R \left[\left(\frac{r^2}{2\beta'^2} - \frac{r_0^2}{2\beta'^2}\right)\right]^{1/\varepsilon} r dr = c_0 \frac{R^2}{2} = \frac{R^2}{2} \tag{A7}$$

which results in:

$$\frac{\varepsilon^{\frac{\varepsilon+1}{\varepsilon}}}{\varepsilon+1} \beta'^2 \left(\frac{R^2}{2\beta'^2} - \frac{r_0^2}{2\beta'^2}\right)^{\frac{\varepsilon+1}{\varepsilon}} = \frac{R^2}{2} \tag{A8}$$

Solving the aforementioned equation for r_0, eq. (13) is finally obtained.

References

1. Yannas, I. V. Tissue and Organ Regeneration in Adults; Springer: NY, 2001.
2. Stevenson, T. R.; Kadhiresan, V. A.; Faulkner, J. A. J Reconstr Microsurg 1994, 10, 171.
3. Harley, B. A.; Yannas, I. V. Minerva Biotechnol 2006, 19, 97.
4. Gibson, K. L.; Remson, L.; Smith, A.; Satterlee, N.; Strain, G. M.; Daniloff, J. K. Microsurgery 1991, 12, 80.
5. Den Dunnen, W. F.; Van Der Lei, B.; Robinson, P. H.; Holwerda, A.; Pennings, A. J.; Schakenraad, J. M. J Biomed Mater Res 1995, 29, 757.
6. Aebischer, P.; Guenard, V.; Valentini, R. F. Brain Res 1990, 531, 211.
7. Rodriguez, F. J.; Gomez, N.; Perego, G.; Navarro, X. Biomaterials 1999, 20, 1489.
8. Chamberlain, L. J.; Yannas, I. V.; Arrizabalaga, A.; Hsu, H. P.; Norregaard, T. V.; Spector, M. Biomaterials 1998, 19, 1393.
9. Jenq, C. B.; Jenq, L. L.; Coggeshall, R. E. Exp Neurol 1987, 97, 662.
10. Jenq, C. B.; Coggeshall, R. E. Brain Res 1987, 408, 239.
11. Aebischer, P.; Guenard, V.; Winn, S. R.; Valentini, R. F.; Galletti, P. M. Brain Res 1988, 454, 179.
12. Chamberlain, L. J.; Yannas, I. V.; Hsu, H. P.; Strichartz, G.; Spector, M. Exp Neurol 1998, 154, 315.
13. Harley, B. A.; Spilker, M. H.; Wu, J. W.; Asano, K.; Hsu, H. P.; Spector, M.; Yannas, I. V. Cells Tissues Organs 2004, 176, 153.
14. Dubey, N.; Letourneau, P. C.; Tranquillo, R. T. Exp Neurol 1999, 158, 338.
15. Oh, S. H.; Lee, J. H. J Biomed Mater Res A 2007, 80, 530.
16. Oh, S. H.; Kim, J. H.; Song, K. S.; Jeon, B. H.; Yoon, J. H.; Seo, T. B.; Namgung, U.; Lee, I. W.; Lee, J. H. Biomaterials 2008, 29, 1601.
17. Chamberlain, L. J.; Yannas, I. V.; Hsu, H. P.; Spector, M. J Comp Neurol 2000, 417, 415.
18. Chamberlain, L. J.; Yannas, I. V.; Hsu, H. P.; Strichartz, G. R.; Spector, M. J Neurosci Res 2000, 60, 666.
19. Spilker, M. H.; Yannas, I. V.; Kostyk, S. K.; Norregaard, T. V.; Hsu, H. P.; Spector, M. Restor Neurol Neurosci 2001, 18, 23.
20. Spilker, M. H. Ph.D. Thesis, Massachusetts Institute of Technology, Cambridge, 2000.
21. Navarro, X.; Rodriguez, F. J.; Labrador, R. O.; Buti, M.; Ceballos, D.; Gomez, N.; Cuadras, J.; Perego, G. J Peripher Nerv Syst 1996, 1, 53.

22. Mackinnon, S. E.; Dellon, A. L. Plast Reconstr Surg 1990, 85, 419.
23. Dellon, A. L.; Mackinnon, S. E. Plast Reconstr Surg 1988, 82, 849.
24. Montgomery, C. T.; Robson, J. A. Exp Neurol 1993, 122, 107.
25. Wake, M. C.; Gupta, P. K.; Mikos, A. G. Cell Transplant 1996, 5, 465.
26. Mooney, D. J.; Mazzoni, C. L.; Breuer, C.; McNamara, K.; Hern, D.; Vacanti, J. P.; Langer, R. Biomaterials 1996, 17, 115.
27. Dalton, P. D.; Flynn, L.; Shoichet, M. S. Biomaterials 2002, 23, 3843.
28. Biesheuvel, P. M.; Nijmeijer, A.; Verweij, H. AIChE J 1998, 44, 1914.
29. Biesheuvel, P. M.; Verweij, H. J Am Ceram Soc 2000, 83, 743.
30. Biesheuvel, P. M.; Breedveld, V.; Higler, A. P.; Verweij, H. Chem Eng Sci 2001, 56, 3517.
31. Harley, B. A.; Hastings, A. Z.; Yannas, I. V.; Sannino, A. Biomaterials 2006, 27, 866.
32. Goraltchouk, A.; Freier, T.; Shoichet, M. S. Biomaterials 2005, 26, 7555.
33. Mironov, V.; Kasyanov, V.; Shu, X. Z.; Eisenberg, C.; Eisenberg, L.; Gonda, S.; Trusk, T.; Markwald, R. R.; Prestwich, G. D. Biomaterials 2005, 26, 7628.
34. Yannas, I. V.; Harley, B. A.; Hastings, A. Z.; Sannino, A. WO Pat. 2006/047758 A1, 2006.
35. Lamm, O. Ark Mat Astr Fys 1929, 21B, 1.
36. Schuck, P. Biophys J 1998, 75, 1503.
37. Cao, W. M.; Demeler, B. Biophys J 2005, 89, 1589.
38. de Gennes, P. G. Scaling Concepts in Polymer Physics; Cornell University Press: Ithaca, NY, 1979.